Alterations in Hippocampal Network Activity after *In Vitro* Traumatic Brain Injury

Woo Hyeun Kang[1], Wenzhe Cao[2], Oliver Graudejus[2, 3], Tapan P. Patel[4], Sigurd Wagner[2], David F. Meaney[4], Barclay Morrison III[1]

Department of Biomedical Engineering, Columbia University[1]

Department of Electrical Engineering, Princeton University[2]

Department of Chemistry and Biochemistry, Arizona State University[3]

Department of Bioengineering, University of Pennsylvania[4]

Forward all correspondence to:

Barclay Morrison III, Ph.D.

Associate Professor

Biomedical Engineering

Columbia University

351 Engineering Terrace, MC 8904

1210 Amsterdam Avenue

New York, NY 10027

Tel: 212-854-6277

Fax: 212-854-8725

Email: bm2119@columbia.edu

Running Title: Reduced Network Synchronization after TBI

Keywords: Traumatic brain injury; hippocampus; network synchronization; electrophysiology

Authors:

Woo Hyeun Kang, MS
Department of Biomedical Engineering
Columbia University
351 Engineering Terrace, MC 8904
1210 Amsterdam Avenue
New York, NY 10027
Tel: 212-854-2823
Fax: 212-854-8725
Email: wk2201@columbia.edu

Wenzhe Cao, PhD
Department of Electrical Engineering
Princeton University

B422 Engineering Quadrangle

41 Olden Street

Princeton, NJ 08540

Tel: 609-258-4631

Fax: 609-258-6279

Email: wcao@princeton.edu

Oliver Graudejus, PhD

Department of Chemistry and Biochemistry

Arizona State University

Interdisciplinary Science and Technology Building I

Tempe, AZ 85287

Tel: 609-532-9744

Email: oliver.graudejus@asu.edu

Tapan Patel, MS

Department of Bioengineering

University of Pennsylvania

240 Skirkanich Hall

210 South 33rd Street

Philadelphia, PA 19104

USA

Tel: (215) 573-3155

Email: tapanp@mail.med.upenn.edu

Sigurd Wagner, PhD

Department of Electrical Engineering

Princeton University

B422 Engineering Quadrangle

41 Olden Street

Princeton, NJ 08540

Tel: 609-258-4631

Fax: 609-258-6279

Email: wagner@princeton.edu

David Meaney, PhD

Department of Bioengineering

University of Pennsylvania

240 Skirkanich Hall

210 South 33rd Street

Philadelphia, PA 19104

USA

Tel: (215) 573-3155

Email: dmeaney@seas.upenn.edu

Abstract

Traumatic brain injury (TBI) alters function and behavior, which can be characterized by changes in electrophysiological function *in vitro*. A common cognitive deficit after mild to moderate TBI is disruption of persistent working memory of which the *in vitro* correlate is long-lasting, neuronal network synchronization that can be induced pharmacologically by the $GABA_A$ antagonist bicuculline. We utilized a novel *in vitro* platform for TBI research, the stretchable microelectrode array (SMEA), to investigate the effects of TBI on bicuculline-induced, long-lasting network synchronization in the hippocampus. Mechanical stimulation significantly

disrupted bicuculline-induced, long-lasting network synchronization 24 hours after injury, despite the continued ability of the injured neurons to fire as revealed by a significant increase in the normalized spontaneous event rate in the dentate gyrus (DG) and CA1. A second challenge with bicuculline 24h after the first significantly decreased the normalized spontaneous event rate in the DG. In addition, we illustrate the utility of the SMEA for TBI research by combining multiple experimental paradigms in one platform, which has the potential to enable novel investigations into the mechanisms responsible for functional consequences of TBI and to speed the rate of drug discovery.

Introduction

Traumatic brain injury (TBI) continues to be a leading cause of death and disability,[1, 2] affecting nearly 10 million people annually worldwide and an estimated 1.7 million people annually in the United States.[3] The devastating behavioral and functional consequences of TBI include cognitive impairment,[4] memory loss or impairment,[5] loss or decreased consciousness,[6] motor deficits,[7] coma,[8] seizure and epilepsy,[9] and death.[10]

Disruption of persistent working memory is a prominent cognitive deficit experienced by individuals with TBI.[11] In adults, the neural correlate for working memory and information storage may be recurrent network activity,[12] which is also involved in neuronal network maturation in the developing brain.[13] In many cases, working memory deficits arise in the absence of cell death or overt structural damage to brain tissue especially in cases of mild or moderate TBI.[14-17]

TBI is caused by deformation of brain tissue, with tissue strain and strain rate identified as significant predictors of injury.[18-21] However, very few studies have characterized *in vivo* tissue strain and strain rate during TBI due to the challenges of directly measuring tissue deformation *in vivo.*[22-24] An *in vitro* approach to these mechanistic studies allows for precise control of the mechanical stimulus and the extracellular environment to examine the response of the brain parenchyma in the absence of systemic influences, while recapitulating much of the *in vivo* pathology.[25, 26]

One way to record *in vitro* neural activity is through the use of microelectrode arrays (MEAs).[17, 27, 28] Compared to single electrode electrophysiological recordings, MEAs enable the investigation of higher order behaviors of neuronal networks comprised of up to many thousands of neurons, due to the ability to record simultaneously from multiple sites.[29, 30] One limitation of available MEAs is their rigid nature, which prevents direct testing of hypotheses relating changes in electrophysiological function to mechanisms of mechanotransduction. Previously, we demonstrated the ability to monitor electrophysiological function in hippocampal slice cultures after mechanical stretch injury using an earlier generation of SMEAs (stretchable microelectrode arrays).[31] In the present study, we leveraged the advantages of the latest generation of SMEA, with more recording electrodes and smaller feature-size, to test our hypothesis that long-lasting, hippocampal network synchronization is disrupted by TBI.

Recurrent network activity or synchronization is regulated by the inhibitory neurotransmitter γ-aminobutyric acid (GABA).[32] Disinhibition, caused by disruptions in GABAergic signaling, may be a leading cause of pathologically persistent activity.[33] Acutely, the $GABA_A$ antagonist bicuculline is used to induce epileptiform bursting activity in brain slice cultures by blocking GABAergic inhibition[34] and to induce long-lasting, recurrent synchronous bursting, hours and days after washout.[28, 35] By utilizing the unique capabilities of the SMEA to combine long-term electrophysiological recording with mechanical stimulation, we investigated the effect of mild to moderate mechanical stretch injury on bicuculline-induced, long-lasting network synchronization.

Our SMEA system has the potential to engender novel experimental strategies to investigate the mechanisms of mechanotransduction underlying the functional consequences of TBI. Compared to more labor intensive *in vivo* approaches, the ability to test TBI hypotheses within a single organotypic slice culture over extended durations could increase the speed of drug discovery through high-content screening.[36]

Materials and Methods

Stretchable microelectrode arrays

Design, fabrication, and packaging of SMEAs have been described previously in detail.[37-39] Briefly, thin-film conductors (3 nm chromium, followed by 75 nm gold, finished with 3 nm chromium) were sequentially deposited on a 280 μm thick layer of polydimethylsiloxane (PDMS, Sylgard 184, Dow Corning, Midland, MI, USA) by electron beam evaporation.[40] The gold thin-film was patterned into recording electrodes and encapsulated with a 15 μm thick layer of either PDMS or photo-patternable silicone (PPS, WL5150, Dow Corning). Vias were opened in the encapsulation layer to expose the recording electrodes and peripheral contacts. Platinum black was electroplated on the surfaces of the recording electrodes. The SMEA was sandwiched between two printed circuit boards with circular openings for the culture well and to allow incorporation into our *in vitro* TBI model.[41] The SMEA featured 28 recording electrodes (feature size < 100 μm), 2 reference electrodes, and 30 peripheral contacts (Figure 1).[38]

Organotypic slice cultures of the rat hippocampus

All animal procedures were approved by the Columbia University Institutional Animal Care and Use Committee (IACUC). Prior to plating organotypic hippocampal slice cultures, SMEAs were made hydrophilic with air gas plasma treatment (Harrick PDC-32G, Harrick Scientific, Pleasantville, NY, USA) for 90 s.[42] SMEAs were pre-coated overnight with 80 μg/mL laminin (Life Technologies, Carlsbad, CA, USA) and 320 μg/mL poly-L-lysine (Sigma-Aldrich, St. Louis, MO, USA), and then incubated overnight with Neurobasal medium (Life Technologies; supplemented with 1 mM Glutamax, 50X B27, 4.5 mg/mL D-glucose, and 10 mM HEPES) in a standard cell-culture incubator (37 °C, 5% CO_2). The brains of post-natal day 8-11 Sprague-Dawley rat pups were aseptically removed, and the hippocampus cut into 375 μm thick slices using a McIlwain tissue chopper (Harvard Apparatus, Holliston, MA, USA) according to published methods.[41] Hippocampal slice cultures were then plated onto pre-coated SMEAs and fed every 2-3 days with conditioned full-serum medium (Sigma-Aldrich; 50% minimum essential media, 25% Hank's balanced salt solution, 25% heat inactivated horse serum, 1 mM Glutamax, 4.5 mg/mL D-glucose, and 10 mM HEPES) for 8-18 days total. To verify slice culture health prior to injury, the fluorescent dye propidium iodide (Life Technologies) was used to stain for dead or injured cells. Unhealthy slice cultures were not included in the study, according to published methods.[43]

Mechanical stretch injury of hippocampal slice cultures

The *in vitro* model of mechanical stretch injury has been characterized previously in detail.[41, 44] Briefly, after 8-18 days *in vitro*, media was removed from the SMEA well, and the hippocampal slice cultures were mechanically stretched by pulling the SMEA over a rigid, tubular indenter. Slice culture electrophysiological function was then assessed as described below. The induced tissue strain and strain rate were verified with high-speed video analysis of the dynamic stretch injury event. Lagrangian strain was determined by calculating the deformation gradient tensor by locating fiducial markers on the tissue slice image before and at maximal stretch.[44]

Assessment of electrophysiological function

At the indicated time point after stretch injury and while still adhered to the SMEA, slice cultures were perfused with artificial cerebrospinal fluid (aCSF, Sigma-Aldrich; 125 mM NaCl, 3.5 mM KCl, 26 mM $NaHCO_3$, 1.2 mM KH_2PO_4, 1.3 mM $MgCl_2$, 2.4 mM $CaCl_2$, 10 mM D-glucose, pH = 7.4) at 37 ℃ and aerated with 95% O_2/5% CO_2, as previously described.[17] For experiments involving GABA inhibition, slice cultures were perfused for a minimum of 3 minutes with bicuculline methiodide 50 μM (Sigma-Aldrich) in aCSF before recording electrical activity, within one hour post-injury. Bicuculline was then washed from the slice cultures for at least 20 minutes before returning them to the incubator for follow-up recordings at the indicated time points.

Spontaneous neural activity was measured by recording continuously for 3 minutes at a sampling rate of 20 kHz from all electrodes within the hippocampus prior to injury and at the indicated time point. Raw data was low pass filtered with a 6 kHz analog, anti-aliasing filter and passed through a 60 Hz comb filter using a custom MATLAB script (version R2012a, MathWorks, Natick, MA, USA). Consistent with other MEA studies with acute slices, the electrodes of the SMEAs recorded the local field potentials produced by populations of neuronal cell bodies, dendrites, and axons within the local vicinity of individual electrodes.[45] Neural event activity was detected based on the multiresolution Teager energy operator (m-TEO), which identifies epochs of data that contain high energy in specific frequency bands that are indicative of the feature being detected.[46] In this case, the feature was the local field potential of neuronal ensembles recorded by the planar electrodes of the SMEA. The m-TEO was calculated for k = (600, 900, 1200), and neural events were identified as the onset of those epochs with an m-TEO greater than 0.5 root-mean-square-error above the baseline m-TEO and with a raw signal greater than 1.5 root-mean-square-error above the baseline of the raw signal.[47]

Using the results from the previous analysis above, which identified the onset time of each neural event on each electrode, the degree of correlation for event trains across electrode pairs was investigated. Spontaneous network synchronization was quantified using previously published methods based on correlation matrix analysis and surrogate resampling for significance testing.[48-50] Correlation of neural events was computed to determine an event synchronization measure, the synchronization index, for each electrode pair.[48] Correlated neural events across electrodes were defined as detected neural events that occurred within 1.5 ms of each other.[47] For two electrodes *x* and *y*, and neural event-timing t_i^x and t_j^y (i = 1, …, m_x; j = 1, …, m_y), the event correlation matrix was calculated by:

$$c^{\tau}(x|y) = \sum_{i=1}^{m_x} \sum_{j=1}^{m_y} J_{ij}^{\tau} \begin{cases} J_{ij}^{\tau} = 1 \; if \; 0 < t_i^x - t_j^y \leq \tau \\ J_{ij}^{\tau} = \frac{1}{2} \; if \; t_i^x = t_j^y \\ J_{ij}^{\tau} = 0 \; otherwise \end{cases} \qquad (1)$$

where τ was the time interval in which two events were considered synchronous (1.5 ms), m_x and m_y were the total number of events to be compared, and J_{ij}^{τ} was a measure of correlation of two particular electrodes.

The event synchronization index for each electrode comparison, ranging in value from 0 (completely uncorrelated) to 1 (perfectly correlated), was calculated by:

$$Q_\tau = \frac{c^\tau(x|y) + c^\tau(y|x)}{\sqrt{m_x m_y}} \tag{2}$$

To identify clusters of synchronized electrodes, first, the participation index (PI) was calculated for each electrode a that contributed to a cluster b:

$$PI_{ab} = \lambda_b v_{ab}^2 \tag{3}$$

where v_{ab} was the a^{th} element of eigenvector v_b and λ_b was the corresponding eigenvalue of the event correlation matrix [$c^\tau(x|y)$]. PI_{ab} indicated the contribution of electrode a to the synchronized cluster b, with v_{ab}^2 defined as the weight with which electrode a contributed to cluster b. Clusters were defined as groups of electrodes with statistically similar patterns of activity, defined by PI ≥ 0.01.[49]

Next, randomized surrogate time-series data without correlated electrode pairs were mathematically generated with an event rate equal to the instantaneous event rate of the experimental recordings by generating an inhomogeneous Poisson-distributed, 'event train.' These uncorrelated, synthetic 'event trains' were analyzed identically to the experimental data to produce a correlation matrix, eigenvalues, eigenvectors, and PI to bootstrap hypothesis testing of the experimental data.[49] Essentially, the uncorrelated Poisson-distributed ‘event trains’ served as the null hypothesis against which to test experimental data. The surrogate randomization was repeated 50 times, and the mean ($\bar{\lambda}'_k$) and standard deviation (SD_k) of surrogate eigenvalues were calculated (k = 1, …, M, where M was the number of electrodes). We identified the number of synchronized clusters that were significantly different from the randomized, asynchronous surrogates by:

$$Number\ of\ Clusters = \sum_k sgn\left[\lambda_k > \left(\bar{\lambda}'_k + K \times SD_k\right)\right] \tag{4}$$

where *sgn* was a sign function, λ_k was the eigenvalue of each electrode of the experimental data, and *K* was a constant (*K* = 3, for 99% confidence level, was used for this study). The detection of synchronized clusters represented the presence of neuronal assemblies functioning in an organized network. It is believed that neuron assemblies play a critical role in higher-order hippocampal function including spatial navigation and memory processes,[51] which may be disrupted after TBI and axonal injury.[52]

The degree of synchronization can be quantified and compared across slice cultures by calculating the global synchronization index (GSI), ranging from 0 (completely random, uncorrelated activity) to 1 (perfectly synchronous, correlated activity), for the cluster with the highest degree of synchronization within each slice culture:

$$GSI = \begin{cases} \dfrac{\lambda_M - \bar{\lambda}'}{M - \bar{\lambda}'} & if\ \lambda_M > \bar{\lambda}' \\ 0 & otherwise \end{cases} \tag{5}$$

where $\bar{\lambda}'$ was the mean of the highest eigenvalues calculated across all surrogates, λ_M was the maximal eigenvalue of the correlation matrix from the experimental data, and M was the number of electrodes. Lower synchronization (i.e. lower GSI) has been associated with dysfunctional or damaged neural networks.[53] Lastly, the GSI was apportioned to each region (DG, CA3, CA1) based on the fraction of regional electrodes participating in the cluster to obtain a normalized GSI for each region.

Statistical Analysis

To account for variability in the density and excitability of neuronal populations at each electrode, spontaneous activity data was normalized to pre-injury levels for neural event rate on an electrode-by-electrode basis. Spontaneous activity and network synchronization data were analyzed by ANOVA, followed by Bonferroni *post hoc* tests with statistical significance set as $p < 0.05$.

Results

Mechanical injury alone did not alter spontaneous network activity

For all injured slice cultures, the average Lagrangian strain was 0.22 ± 0.02 and the average strain rate was $2.37 \pm 0.39\ s^{-1}$ ($n = 12$ slice cultures, mean $\pm$ SD), which constituted a mild to moderate injury as previously reported.[17-19] Cell death was consistent with previously reported cell death in hippocampal slice cultures caused by mild to moderate injury.[19] Immediately post-injury and 24 hours after injury, no significant change in the normalized GSI was observed in any region (Figure 2A). In addition, no significant alterations in the normalized spontaneous event rate were observed in any region either acutely or 24 hours after injury (Figure 2B). These results are consistent with the mild to moderate severity of the injury and the recording time point.[17, 31]

Mechanical injury disrupted bicuculline-induced, long-lasting network synchronization

In both uninjured and injured slice cultures, bicuculline induced highly synchronized, correlated neural activity (Figure 3A, B). Prior to injury or bicuculline treatment, the hippocampal network was not synchronized as denoted by low (blue) correlation coefficients (Figure 4A, D). During bicuculline treatment, network synchronization increased in both uninjured and injured slice cultures (Figure 4B, E). 24 hours after bicuculline treatment, the hippocampal network remained highly synchronized in uninjured slice cultures (Figure 4C), whereas in injured cultures synchrony was significantly decreased (Figure 4F).

Before injury or bicuculline treatment, the normalized GSI was very low in all regions of both uninjured and injured slice cultures (Figure 5, normalized GSI < 0.01). During bicuculline treatment, the normalized GSI significantly increased in all regions in both uninjured and injured cultures. 24 hours after bicuculline treatment, the normalized GSI was significantly higher in uninjured cultures compared to pre-bicuculline levels and compared to injured cultures. In contrast, in all regions of injured cultures, the normalized GSI was significantly decreased compared to during bicuculline treatment.

Mechanical injury increased the rate of bicuculline-induced spontaneous activity

In all regions of uninjured slice cultures, no significant alteration in the normalized spontaneous event rate was observed 24 hours after bicuculline exposure (Figure 6A, B, C). However, 24 hours after bicuculline exposure of injured slice cultures, the normalized spontaneous event rate was significantly increased in the DG and CA1 compared to pre-injury, pre-treatment levels, as well as when compared to uninjured cultures at the same time point (Figure 6A, C). No significant changes were observed in CA3 (Figure 6B). These results suggest that mild to moderate injury affected the ability of the surviving neuronal network to synchronize activity and not simply the ability of neurons to generate activity.

Effects of bicuculline re-exposure differed by hippocampal region

24 hours after the initial bicuculline treatment, injured slice cultures were exposed to bicuculline a second time to probe for potential mechanisms of the disruption in bicuculline-induced, long-lasting network synchronization. Re-exposure to bicuculline significantly increased the normalized GSI in all hippocampal regions compared to pre-injury, pre-treatment baseline levels and compared to 24 hours after the initial post-injury bicuculline exposure (Figure 7A). In contrast, the effect of re-exposure to bicuculline on event rate was region-dependent, significantly decreasing spontaneous activity in the DG but significantly increasing it in CA3 and CA1 (Figure 7B).

Discussion

In the present study, bicuculline exposure almost immediately transformed the network activity of both uninjured and injured hippocampal slice cultures from random, asynchronous activity to highly synchronized, correlated neural activity (Figure 3). In uninjured cultures, this coordinated activity persisted for at least 24 hours after the removal of bicuculline (Figure 4). In contrast, this long-lasting network synchronization was not evident in cultures that were mechanically injured (Figure 5A-C), despite increased network synchronization during bicuculline exposure and despite increased asynchronous activity 24h after bicuculline exposure (Figure 6A-C).

The injury severity for this study was chosen to be characteristic of mild to moderate TBI, which causes neuronal network dysfunction without appreciable cell death.[17] We observed that mechanical injury disrupted bicuculline-induced, long-lasting network synchronization, but did not abolish neuronal network activity (Figures 4-6). In fact, the normalized spontaneous event rate was higher in the DG and CA1 24 hours after injury (Figure 6A, 6C). Despite the hippocampal neuronal network being even more active after injury, it was unable to maintain synchronized, correlated activity, a deficit that could explain learning and memory impairments after TBI because the neural process underlying information storage in working memory is persistent neural activity.[12] During memory encoding and recognition, optimally functional neuronal networks are highly organized and exhibit synchronization between interconnected neuronal regions.[54] Brain dysfunction after injury, such as mild TBI,[53] or as a result of neurological disorders, such as Alzheimer's disease,[55] alters the functional structure of neuronal networks, transforming synchronized networks into less ordered and more random networks. In patients tested within days of suffering a mild TBI, global synchronization and network organization of rhythmic brain activity hypothesized to underlie episodic memory, was reduced, as measured by electroencephalography (EEG) recordings.[53] These patients also exhibited reduced performance in visual recognition tasks that were dependent on short-term episodic memory. It is an interesting observation that, in the current study, stretch disrupted the development of long-lasting network synchronization *in vitro*, as well.[53]

Exposing injured slice cultures to a second bicuculline challenge 24 hours after the initial exposure resulted in region-dependent changes in the normalized event rate (Figure 7). We speculate that the underlying mechanism behind this region-dependent observation may involve the interplay between the K-Cl co-transporter (KCC2) and the Na-K-2Cl co-transporter (NKCC1) in regulating the concentration of intracellular chloride. KCC2 has been implicated to play a key role in the impairment of GABAergic inhibition after mechanical injury.[56] Bonislawski *et al*. observed significantly reduced KCC2 expression after TBI and a concomitant depolarized shift of the normally hyperpolarizing $GABA_A$ reversal potential in DG, but not CA1. Additionally, in a separate study, significant enhancement of spontaneous circuit activity in cultured hippocampal neurons was observed after pharmacological inhibition of KCC2.[57] With the depolarizing shift in the $GABA_A$ reversal potential due to post-injury alterations in KCC2 expression, GABA neurotransmission may become depolarizing/excitatory rather than hyperpolarizing/inhibitory, thereby increasing spontaneous activity after injury. In this case, inhibition of GABA by bicuculline would then be hypothesized to decrease spontaneous activity, which may help explain our observations in the DG after injury (Figure 7). In general, however, chloride gradients shift by changing the expression of NKCC1 and KCC2 in the 2nd week of development in rodents.[58] The hippocampal slice cultures used in our experiments were generated from P8-11 rat pups and were further cultured for an additional 18 days. Future experiments will be necessary to directly test whether changes in expression or activity of KCC2 and NKCC1 are responsible for these post-traumatic changes in network function. Quantifying the changes in NKCC1 and KCC2 protein expression before and after injury may uncover region-dependent roles of the chloride transporters within the hippocampus.

Significant progress has been made in improving the fabrication process of the SMEA and reducing the size of the recording contacts from 300 µm x 300 µm to 100 µm x 100 µm, nearly 90% smaller compared to earlier generations.[38] The reduced feature size has allowed for an increase in the number of recording electrodes from 11 to 28 (12 to 30 electrodes total, including reference electrodes) over the same surface area. However, a continuing limitation of the SMEA is the relatively large feature size of the recording electrodes compared to individual neurons. Commercially available rigid MEAs feature electrodes as small as 8 µm in diameter (256MEA30/8iR-ITO, Multichannel Systems). Currently, multiple neurons and neuronal ensembles may contribute to the summed signal measured from a single electrode. Smaller electrodes could potentially allow for stimulation and recording of individual neurons, increasing the spatial resolution of SMEA-based studies. Although the fabrication process remains difficult and expensive, efforts are underway to improve it and reduce overall manufacturing costs. In addition, *in vitro* slice cultures do not precisely recapitulate important factors of the *in vivo* extracellular environment, such as oxygenation and interplay with systemic blood supply.[25] Components of these systemic factors can be added to an *in vitro* slice culture model, but would require further characterization in order to limit any confounding effects.

Acknowledgments

This work was supported in part by the National Highway Traffic Safety Administration (DTNH22-08-C-00088), the New Jersey Commission on Brain Injury Research (08-3209-BIR-

E-1), and by a Multidisciplinary University Research Initiative from the Army Research Office (W911MF-10-1-0526). The authors gratefully acknowledge the pioneering efforts of Stephanie P. Lacour (EPFL) in the early development of the SMEA.

References

1. Gean, A.D. and Fischbein, N.J. (2010). Head trauma. Neuroimaging clinics of North America 20, 527-556.

2. Hyder, A.A., Wunderlich, C.A., Puvanachandra, P., Gururaj, G. and Kobusingye, O.C. (2007). The impact of traumatic brain injuries: a global perspective. NeuroRehabilitation 22, 341-353.

3. Faul, M., Xu, L., Wald, M.M., Coronado, V. and Dellinger, A.M. (2010). Traumatic Brain Injury in the United States: National Estimates of Prevalence and Incidence, 2002-2006. Injury Prev 16, A268-A268.

4. Kinnunen, K.M., Greenwood, R., Powell, J.H., Leech, R., Hawkins, P.C., Bonnelle, V., Patel, M.C., Counsell, S.J. and Sharp, D.J. (2011). White matter damage and cognitive impairment after traumatic brain injury. Brain 134, 449-463.

5. Christidi, F., Bigler, E.D., McCauley, S.R., Schnelle, K.P., Merkley, T.L., Mors, M.B., Li, X., Macleod, M., Chu, Z., Hunter, J.V., Levin, H.S., Clifton, G.L. and Wilde, E.A. (2011). Diffusion tensor imaging of the perforant pathway zone and its relation to memory function in patients with severe traumatic brain injury. J Neurotrauma 28, 711-725.

6. Ommaya, A.K. and Gennarelli, T.A. (1974). Cerebral concussion and traumatic unconsciousness. Correlation of experimental and clinical observations of blunt head injuries. Brain 97, 633-654.

7. Fujimoto, S.T., Longhi, L., Saatman, K.E., Conte, V., Stocchetti, N. and McIntosh, T.K. (2004). Motor and cognitive function evaluation following experimental traumatic brain injury. Neuroscience and biobehavioral reviews 28, 365-378.

8. Margulies, S.S. and Thibault, L.E. (1989). An analytical model of traumatic diffuse brain injury. J Biomech Eng 111, 241-249.

9. Asikainen, I., Kaste, M. and Sarna, S. (1999). Early and late posttraumatic seizures in traumatic brain injury rehabilitation patients: brain injury factors causing late seizures and influence of seizures on long-term outcome. Epilepsia 40, 584-589.

10. Sosin, D.M., Sniezek, J.E. and Waxweiler, R.J. (1995). Trends in death associated with traumatic brain injury, 1979 through 1992. Success and failure. JAMA 273, 1778-1780.

11. Hoskison, M.M., Moore, A.N., Hu, B., Orsi, S., Kobori, N. and Dash, P.K. (2009). Persistent working memory dysfunction following traumatic brain injury: evidence for a time-dependent mechanism. Neuroscience 159, 483-491.

12. Wang, X.J. (2001). Synaptic reverberation underlying mnemonic persistent activity. Trends Neurosci 24, 455-463.

13. Buzsaki, G. (1989). Two-stage model of memory trace formation: a role for "noisy" brain states. Neuroscience 31, 551-570.

14. Kobori, N. and Dash, P.K. (2006). Reversal of brain injury-induced prefrontal glutamic acid decarboxylase expression and working memory deficits by D1 receptor antagonism. J Neurosci 26, 4236-4246.

15. Levin, H.S., Hanten, G., Chang, C.C., Zhang, L., Schachar, R., Ewing-Cobbs, L. and Max, J.E. (2002). Working memory after traumatic brain injury in children. Ann Neurol 52, 82-88.

16. McAllister, T.W., Saykin, A.J., Flashman, L.A., Sparling, M.B., Johnson, S.C., Guerin, S.J., Mamourian, A.C., Weaver, J.B. and Yanofsky, N. (1999). Brain activation during working memory 1 month after mild traumatic brain injury: a functional MRI study. Neurology 53, 1300-1308.

17. Yu, Z. and Morrison, B., 3rd (2010). Experimental mild traumatic brain injury induces functional alteration of the developing hippocampus. J Neurophysiol 103, 499-510.

18. Elkin, B.S. and Morrison, B., 3rd (2007). Region-specific tolerance criteria for the living brain. Stapp Car Crash J 51, 127-138.

19. Cater, H.L., Sundstrom, L.E. and Morrison, B., 3rd (2006). Temporal development of hippocampal cell death is dependent on tissue strain but not strain rate. J Biomech 39, 2810-2818.

20. Viano, D.C., Casson, I.R., Pellman, E.J., Zhang, L., King, A.I. and Yang, K.H. (2005). Concussion in professional football: brain responses by finite element analysis: part 9. Neurosurgery 57, 891-916; discussion 891-916.

21. Kleiven, S. (2007). Predictors for traumatic brain injuries evaluated through accident reconstructions. Stapp Car Crash J 51, 81-114.

22. Hardy, W.N., Mason, M.J., Foster, C.D., Shah, C.S., Kopacz, J.M., Yang, K.H., King, A.I., Bishop, J., Bey, M., Anderst, W. and Tashman, S. (2007). A study of the response of the human cadaver head to impact. Stapp Car Crash J 51, 17-80.

23. Bayly, P.V., Cohen, T.S., Leister, E.P., Ajo, D., Leuthardt, E.C. and Genin, G.M. (2005). Deformation of the human brain induced by mild acceleration. J Neurotrauma 22, 845-856.

24. Bayly, P.V., Black, E.E., Pedersen, R.C., Leister, E.P. and Genin, G.M. (2006). In vivo imaging of rapid deformation and strain in an animal model of traumatic brain injury. J Biomech 39, 1086-1095.

25. Morrison, B., 3rd, Elkin, B.S., Dolle, J.P. and Yarmush, M.L. (2011). In vitro models of traumatic brain injury. Annu Rev Biomed Eng 13, 91-126.

26. Morrison, B., 3rd, Saatman, K.E., Meaney, D.F. and McIntosh, T.K. (1998). In vitro central nervous system models of mechanically induced trauma: a review. J Neurotrauma 15, 911-928.

27. Beggs, J.M. and Plenz, D. (2004). Neuronal avalanches are diverse and precise activity patterns that are stable for many hours in cortical slice cultures. J Neurosci 24, 5216-5229.

28. Arnold, F.J., Hofmann, F., Bengtson, C.P., Wittmann, M., Vanhoutte, P. and Bading, H. (2005). Microelectrode array recordings of cultured hippocampal networks reveal a simple model for transcription and protein synthesis-dependent plasticity. J Physiol 564, 3-19.

29. Kralik, J.D., Dimitrov, D.F., Krupa, D.J., Katz, D.B., Cohen, D. and Nicolelis, M.A. (2001). Techniques for long-term multisite neuronal ensemble recordings in behaving animals. Methods 25, 121-150.

30. Doetsch, G.S. (2000). Patterns in the brain. Neuronal population coding in the somatosensory system. Physiol Behav 69, 187-201.

31. Yu, Z., Graudejus, O., Tsay, C., Lacour, S.P., Wagner, S. and Morrison, B., 3rd (2009). Monitoring hippocampus electrical activity in vitro on an elastically deformable microelectrode array. J Neurotrauma 26, 1135-1145.

32. Matsuyama, S., Taniguchi, T., Kadoyama, K. and Matsumoto, A. (2008). Long-term potentiation-like facilitation through GABAA receptor blockade in the mouse dentate gyrus in vivo. Neuroreport 19, 1809-1813.

33. Sloviter, R.S. (1994). On the relationship between neuropathology and pathophysiology in the epileptic hippocampus of humans and experimental animals. Hippocampus 4, 250-253.

34. De Curtis, M., Biella, G., Forti, M. and Panzica, F. (1994). Multifocal spontaneous epileptic activity induced by restricted bicuculline ejection in the piriform cortex of the isolated guinea pig brain. J Neurophysiol 71, 2463-2476.

35. Li, X., Zhou, W., Zeng, S., Liu, M. and Luo, Q. (2007). Long-term recording on multi-electrode array reveals degraded inhibitory connection in neuronal network development. Biosens Bioelectron 22, 1538-1543.

36. Sundstrom, L., Morrison, B., 3rd, Bradley, M. and Pringle, A. (2005). Organotypic cultures as tools for functional screening in the CNS. Drug Discov Today 10, 993-1000.

37. Lacour, S.P., Wagner, S., Huang, Z.Y. and Suo, Z. (2003). Stretchable gold conductors on elastomeric substrates. Appl Phys Lett 82, 2404-2406.

38. Graudejus, O., Morrison, B., Goletiani, C., Yu, Z. and Wagner, S. (2012). Encapsulating Elastically Stretchable Neural Interfaces: Yield, Resolution, and Recording/Stimulation of Neural Activity. Adv Funct Mater 22, 640-651.

39. Tsay, C., Lacour, S.P., Wagner, S. and Morrison, B. (2005). Architecture, fabrication, and properties of stretchable micro-electrode arrays. Proc. 4th IEEE Conf. Sensors, 1169-1172.

40. Graudejus, O., Yu, Z., Jones, J., Morrison, B. and Wagner, S. (2009). Characterization of an Elastically Stretchable Microelectrode Array and Its Application to Neural Field Potential Recordings. J Electrochem Soc 156, P85-P94.

41. Morrison, B., 3rd, Cater, H.L., Benham, C.D. and Sundstrom, L.E. (2006). An in vitro model of traumatic brain injury utilising two-dimensional stretch of organotypic hippocampal slice cultures. J Neurosci Methods 150, 192-201.

42. Egert, U. and Meyer, T. (2005). Heart on a Chip — Extracellular Multielectrode Recordings from Cardiac Myocytes in Vitro. In: *Practical Methods in Cardiovascular Research*. Dhein, S., Mohr, F., Delmar, M. (eds). Springer Berlin Heidelberg, pps. 432-453.

43. Effgen, G.B., Hue, C.D., Vogel, E., 3rd, Panzer, M.B., Meaney, D.F., Bass, C.R. and Morrison, B., 3rd (2012). A Multiscale Approach to Blast Neurotrauma Modeling: Part II: Methodology for Inducing Blast Injury to in vitro Models. Frontiers in neurology 3, 23.

44. Morrison, B., 3rd, Cater, H.L., Wang, C.C., Thomas, F.C., Hung, C.T., Ateshian, G.A. and Sundstrom, L.E. (2003). A tissue level tolerance criterion for living brain developed with an in vitro model of traumatic mechanical loading. Stapp Car Crash J 47, 93-105.

45. Novak, J.L. and Wheeler, B.C. (1988). Multisite hippocampal slice recording and stimulation using a 32 element microelectrode array. J Neurosci Methods 23, 149-159.

46. Choi, J.H., Jung, H.K. and Kim, T. (2006). A new action potential detector using the MTEO and its effects on spike sorting systems at low signal-to-noise ratios. IEEE Trans Biomed Eng 53, 738-746.

47. Pimashkin, A., Kastalskiy, I., Simonov, A., Koryagina, E., Mukhina, I. and Kazantsev, V. (2011). Spiking signatures of spontaneous activity bursts in hippocampal cultures. Frontiers in computational neuroscience 5, 46.

48. Li, X., Cui, D., Jiruska, P., Fox, J.E., Yao, X. and Jefferys, J.G. (2007). Synchronization measurement of multiple neuronal populations. J Neurophysiol 98, 3341-3348.

49. Li, X., Ouyang, G., Usami, A., Ikegaya, Y. and Sik, A. (2010). Scale-free topology of the CA3 hippocampal network: a novel method to analyze functional neuronal assemblies. Biophys J 98, 1733-1741.

50. Patel, T.P., Ventre, S.C. and Meaney, D.F. (2012). Dynamic changes in neural circuit topology following mild mechanical injury in vitro. Ann Biomed Eng 40, 23-36.

51. Bahner, F., Weiss, E.K., Birke, G., Maier, N., Schmitz, D., Rudolph, U., Frotscher, M., Traub, R.D., Both, M. and Draguhn, A. (2011). Cellular correlate of assembly formation in oscillating hippocampal networks in vitro. Proc Natl Acad Sci U S A 108, E607-616.

52. Sharp, D.J., Scott, G. and Leech, R. (2014). Network dysfunction after traumatic brain injury. Nat Rev Neurol 10, 156-166.

53. Tsirka, V., Simos, P.G., Vakis, A., Kanatsouli, K., Vourkas, M., Erimaki, S., Pachou, E., Stam, C.J. and Micheloyannis, S. (2011). Mild traumatic brain injury: graph-model characterization of brain networks for episodic memory. Int J Psychophysiol 79, 89-96.

54. Stam, C.J., Jones, B.F., Nolte, G., Breakspear, M. and Scheltens, P. (2007). Small-world networks and functional connectivity in Alzheimer's disease. Cereb Cortex 17, 92-99.

55. Stam, C.J., de Haan, W., Daffertshofer, A., Jones, B.F., Manshanden, I., van Cappellen van Walsum, A.M., Montez, T., Verbunt, J.P., de Munck, J.C., van Dijk, B.W., Berendse, H.W. and Scheltens, P. (2009). Graph theoretical analysis of magnetoencephalographic functional connectivity in Alzheimer's disease. Brain 132, 213-224.

56. Bonislawski, D.P., Schwarzbach, E.P. and Cohen, A.S. (2007). Brain injury impairs dentate gyrus inhibitory efficacy. Neurobiol Dis 25, 163-169.

57. Wang, W. and Xu, T.L. (2006). Chloride homeostasis differentially affects GABA(A) receptor- and glycine receptor-mediated effects on spontaneous circuit activity in hippocampal cell culture. Neurosci Lett 406, 11-16.

58. Leinekugel, X., Khalilov, I., McLean, H., Caillard, O., Gaiarsa, J.L., Ben-Ari, Y. and Khazipov, R. (1999). GABA is the principal fast-acting excitatory transmitter in the neonatal brain. Adv Neurol 79, 189-201.

59. Cramer, S.W., Baggott, C., Cain, J., Tilghman, J., Allcock, B., Miranpuri, G., Rajpal, S., Sun, D. and Resnick, D. (2008). The role of cation-dependent chloride transporters in neuropathic pain following spinal cord injury. Mol Pain 4, 36.

60. Hasbargen, T., Ahmed, M.M., Miranpuri, G., Li, L., Kahle, K.T., Resnick, D. and Sun, D. (2010). Role of NKCC1 and KCC2 in the development of chronic neuropathic pain following spinal cord injury. Ann N Y Acad Sci 1198, 168-172.

61. Mao, X., Ji, C., Sun, C., Cao, D., Ma, P., Ji, Z., Cao, F., Min, D., Li, S., Cai, J. and Cao, Y. (2012). Topiramate attenuates cerebral ischemia/reperfusion injury in gerbils via activating GABAergic signaling and inhibiting astrogliosis. Neurochem Int 60, 39-46.

62. Dai, J., Chen, L., Qiu, Y.M., Li, S.Q., Xiong, W.H., Yin, Y.H., Jia, F. and Jiang, J.Y. (2013). Activations of GABAergic signaling, HSP70 and MAPK cascades are involved in baicalin's neuroprotection against gerbil global ischemia/reperfusion injury. Brain Res Bull 90, 1-9.

63. Shulga, A., Thomas-Crusells, J., Sigl, T., Blaesse, A., Mestres, P., Meyer, M., Yan, Q., Kaila, K., Saarma, M., Rivera, C. and Giehl, K.M. (2008). Posttraumatic GABA(A)-mediated [Ca2+]i increase is essential for the induction of brain-derived neurotrophic factor-dependent survival of mature central neurons. J Neurosci 28, 6996-7005.

64. Gahwiler, B.H., Capogna, M., Debanne, D., McKinney, R.A. and Thompson, S.M. (1997). Organotypic slice cultures: a technique has come of age. Trends Neurosci 20, 471-477.

65. Kovacs, K., Basu, K., Rouiller, I. and Sik, A. (2014). Regional differences in the expression of K(+)-Cl (-) 2 cotransporter in the developing rat cortex. Brain structure & function 219, 527-538.

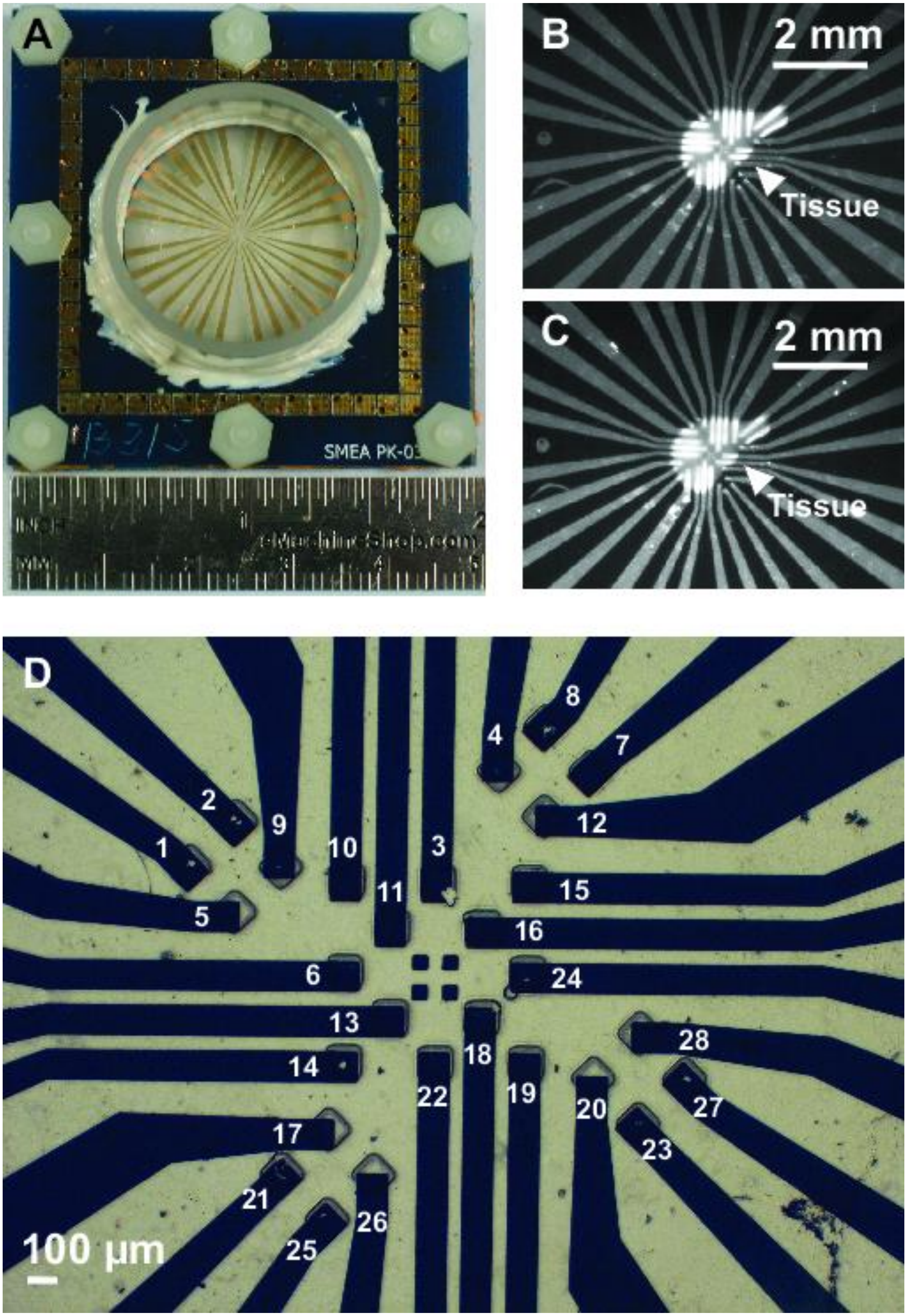
A
SMEA PK-03
B
2 mm
Tissue
C
2 mm
Tissue
D
1
2
3
4
5
6
7
8
9
10
11
12
13
14
15
16
17
18
19
20
21
22
23
24
25
26
27
28
100 µm

Figure 1. Images of an SMEA. (A) The SMEA featured 28 electrodes and 2 reference electrodes in a 49 mm x 49 mm package. (B) Image of a hippocampal slice culture on an SMEA before stretch injury. (C) Image of a hippocampal slice culture on an SMEA after stretch injury of approximately 0.2 strain and 2 s^{-1} strain rate. (D) Image of the 28-electrode array in the center of the SMEA. The tips of the patterned conductors were exposed through 100 μm x 100 μm vias photopatterned in the encapsulation layer. The four small squares in the center are registration marks for aligning photolithographic masks. Individual electrode ID assignments are indicated in white.

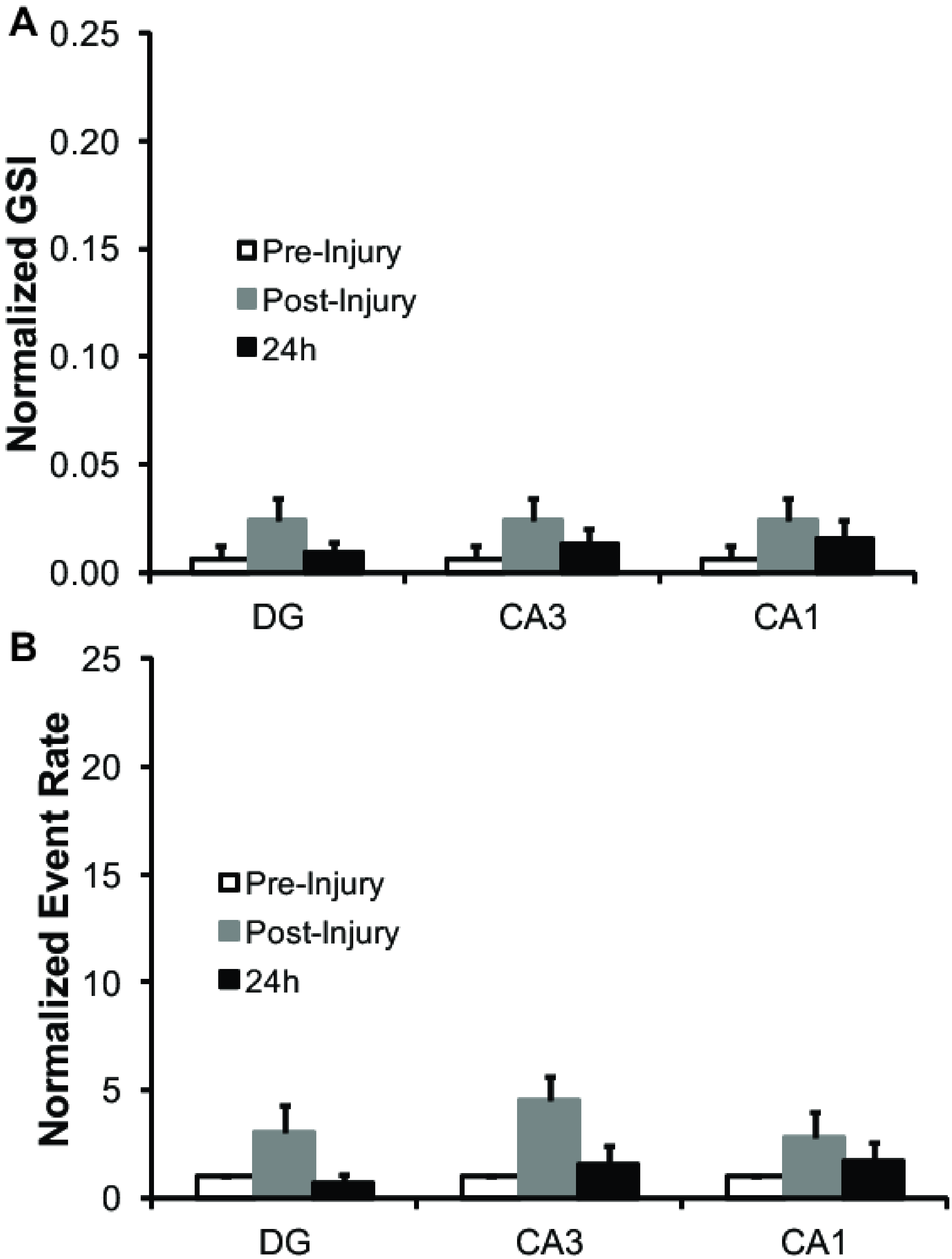
A
0.25
0.20
0.15
0.10
0.05
0.00
Normalized GSI
Pre-Injury
Post-Injury
24h
DG
CA3
CA1
B
25
20
15
10
5
0
Normalized Event Rate
Pre-Injury
Post-Injury
24h
DG
CA3
CA1

Figure 2. Neither network synchronization of spontaneous activity nor the normalized spontaneous event rate was significantly affected by injury. (A) Network synchronization, as measured by the normalized global synchronization index (GSI), was not significantly affected by injury either acutely or 24 hours after injury in DG, CA3, or CA1. (B) The normalized spontaneous event rate was not significantly altered by injury in DG, CA3, or CA1, either acutely after injury or 24 hours after injury. All data was normalized to pre-injury, pre-treatment levels (mean $\pm$ SEM).

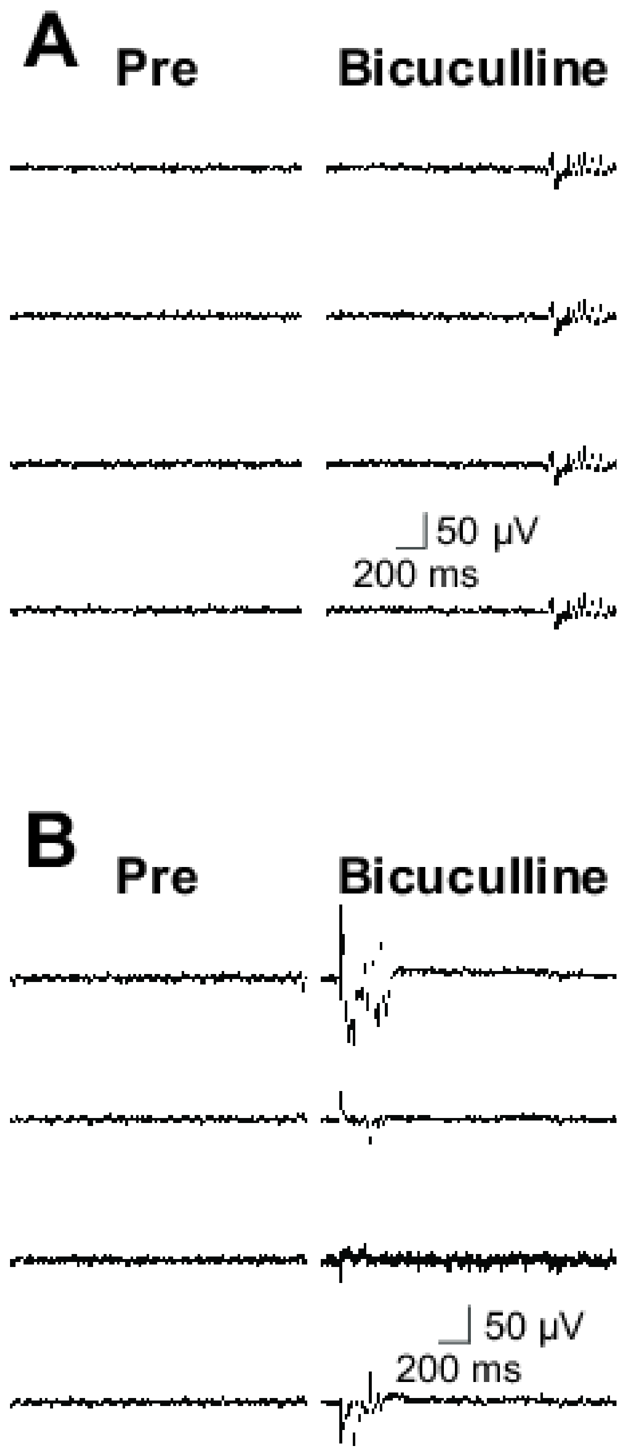
A
Pre
Bicuculline
50 µV
200 ms
B
Pre
Bicuculline
50 µV
200 ms

Figure 3. Representative traces of temporally aligned raw electrophysiology data from 4 electrodes in CA1 before bicuculline treatment and during bicuculline treatment from uninjured (A) and injured (B) slice cultures.

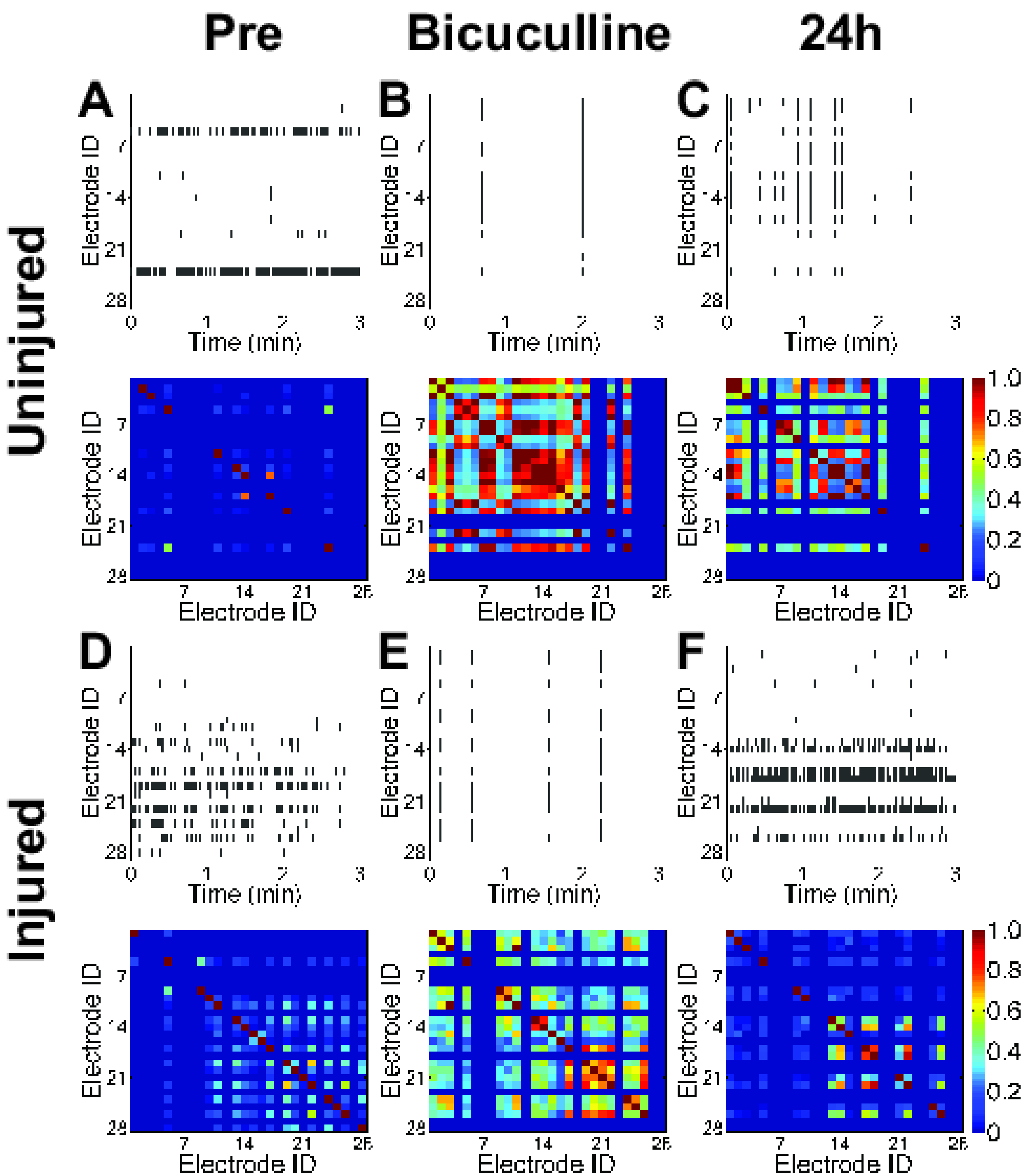

Figure 4. Changes in bicuculline-induced, long-lasting network synchronization of spontaneous activity in uninjured and injured slice cultures. Representative raster plots of spontaneous

activity and heat maps of pair-wise synchronization $c^{\tau}(x|y)$ for every electrode pair are shown for uninjured and injured slice cultures at the indicated time points: before injury (or sham exposure) and before bicuculline treatment (A, D), during bicuculline treatment (B, E), and 24 hours after bicuculline treatment (C, F). Each line in the raster plots represent a distinct, identified neural event. Heat maps of pair-wise synchronization depict the event synchronization index for each electrode pair, ranging in value from 0 (completely uncorrelated, blue) to 1 (perfectly correlated, red).

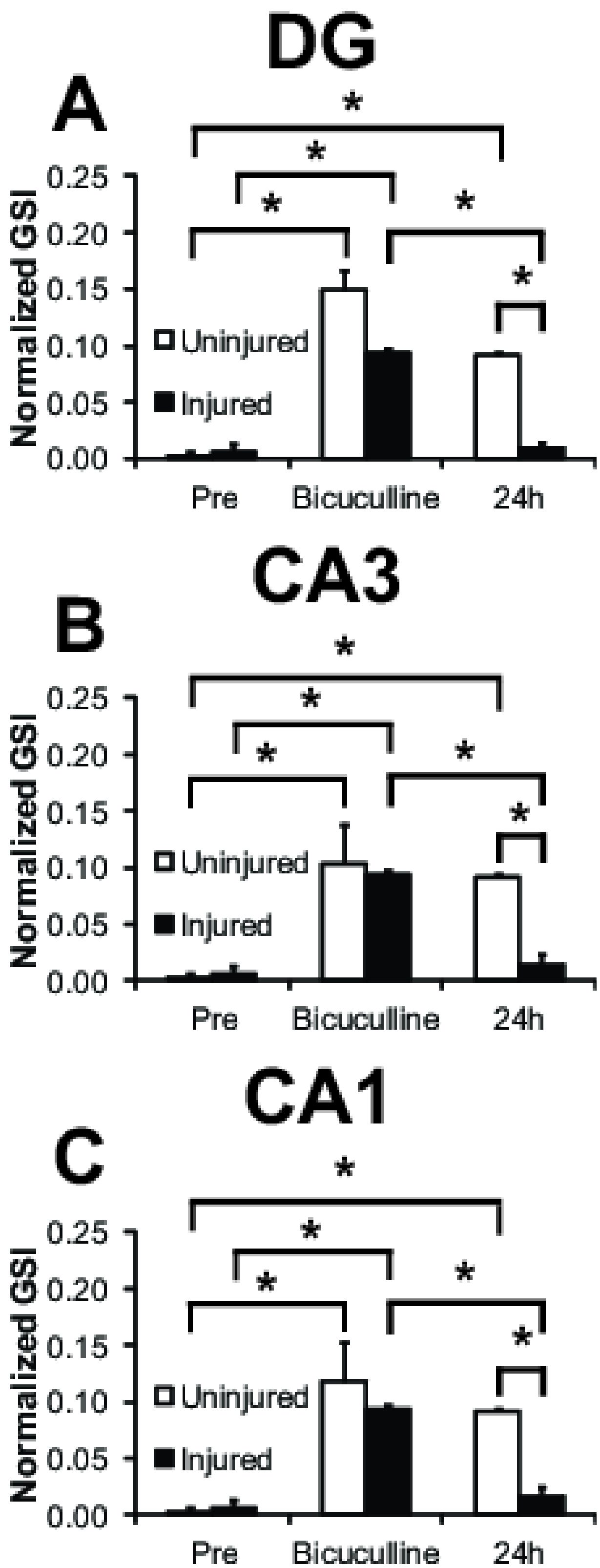
DG
A
CA3
B
CA1
C
Normalized GSI
0.25
0.20
0.15
0.10
0.05
0.00
Uninjured
Injured
Pre
Bicuculline
24h

Figure 5. Changes in bicuculline-induced, long-lasting network synchronization of spontaneous activity in uninjured and injured slice cultures, quantified by the normalized GSI. Before injury (or sham exposure) and bicuculline treatment, network activity was not synchronized in any region (DG, CA3, or CA1), with the normalized GSI below 0.01 (A, B, C). Acutely during bicuculline exposure, the normalized GSI increased significantly in all hippocampal regions in both uninjured and injured slice cultures, compared to their respective baseline recordings, indicating significantly higher network synchronization. 24 hours after bicuculline exposure, the normalized GSI remained significantly higher in all hippocampal regions in uninjured slice cultures compared to pre-treatment baseline levels. In all regions of injured slice cultures, the normalized GSI was significantly diminished 24 hours after bicuculline exposure when compared to the normalized GSI during bicuculline treatment, and when compared to uninjured slice cultures 24 hours after bicuculline treatment. Data is presented as mean $\pm$ SEM.

3

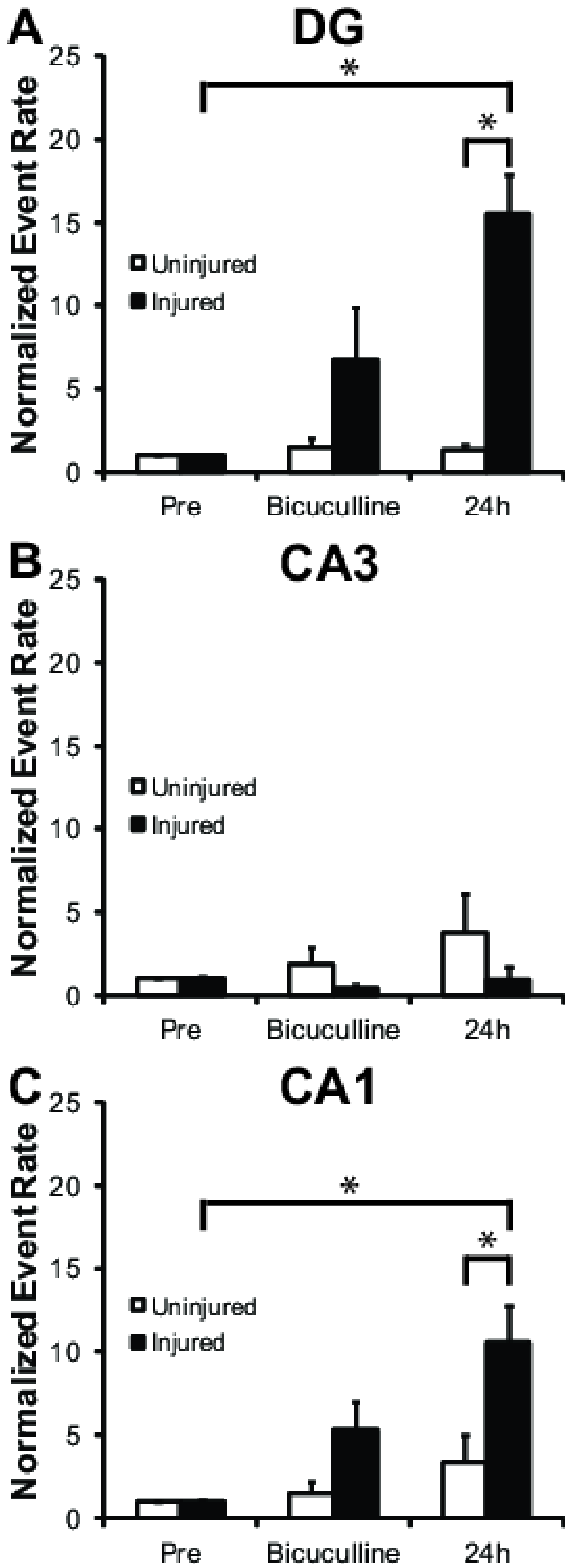
A
DG
B
CA3
C
CA1
Normalized Event Rate
25
20
15
10
5
0
Uninjured
Injured
*
Pre
Bicuculline
24h

4

Figure 6. The normalized spontaneous event rate before and after bicuculline treatment in uninjured and injured slice cultures. 24 hours after bicuculline exposure, the normalized spontaneous event rate was significantly increased in injured DG (A) and CA1 (C) compared to pre-treatment, pre-injury baseline levels and compared to uninjured DG and CA1 at the same time point. No significant changes in the normalized spontaneous event rate were observed in CA3 (B). All data was normalized to pre-injury, pre-treatment levels (mean $\pm$ SEM).

13

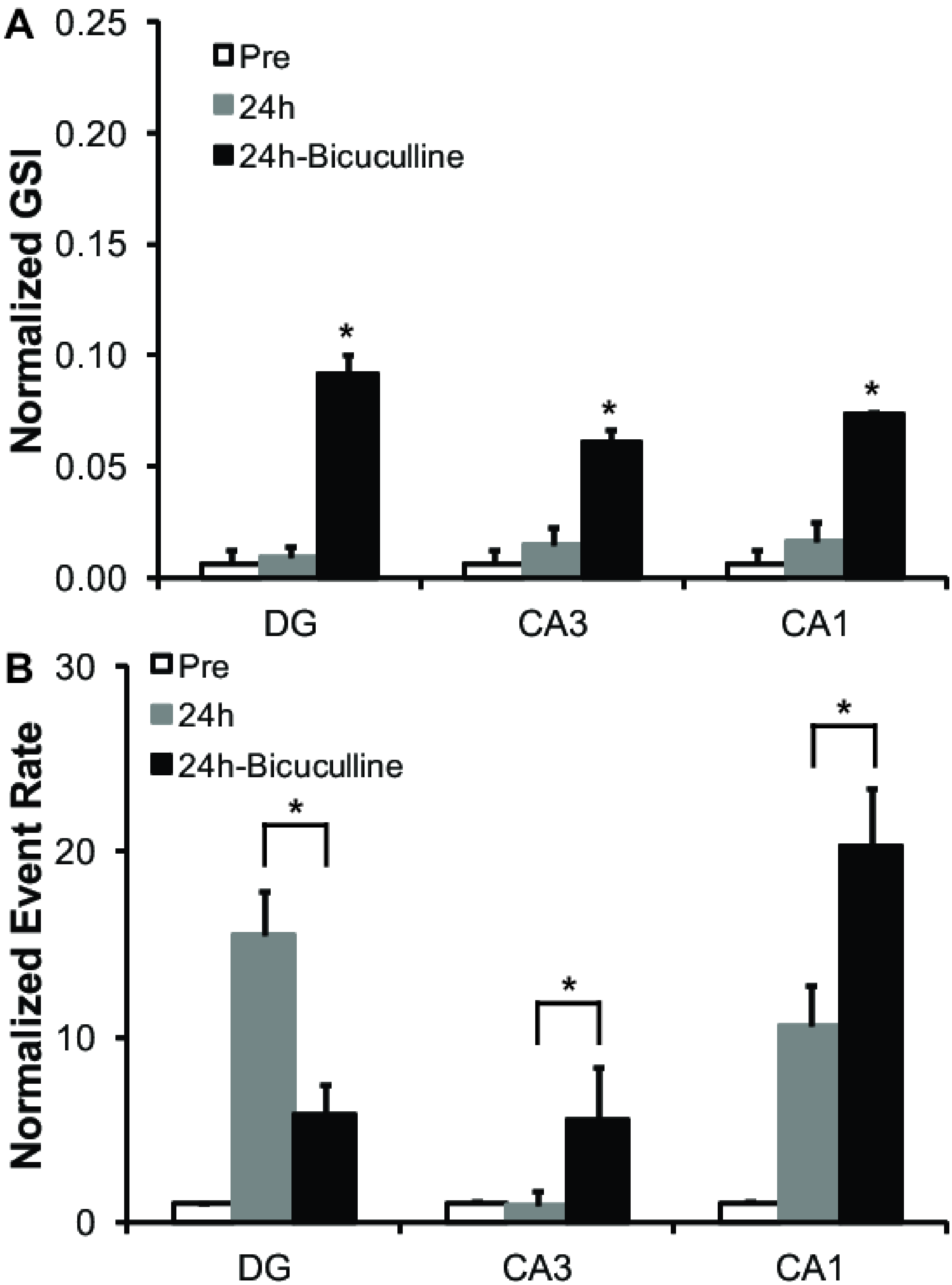
A
0.25
0.20
0.15
0.10
0.05
0.00
Normalized GSI
Pre
24h
24h-Bicuculline
*
DG
CA3
CA1
B
30
20
10
0
Normalized Event Rate
Pre
24h
24h-Bicuculline
*
DG
CA3
CA1

14

Figure 7. Changes in network synchronization of spontaneous activity and the normalized spontaneous event rate in injured slice cultures. (A) A second exposure to bicuculline 24 hours after the initial bicuculline exposure significantly increased the normalized GSI compared to pre-injury, pre-treatment baseline levels and compared to 24 hours after injury and the initial bicuculline exposure in DG, CA3, and CA1. The normalized GSI was not significantly different between hippocampal regions after the second bicuculline exposure. (B) A second exposure to bicuculline 24 hours after the initial bicuculline exposure produced different effects on the normalized spontaneous event rate depending on hippocampal region. Compared to 24h, re-exposure to bicuculline significantly decreased the normalized spontaneous event rate in DG, while significantly increasing the normalized spontaneous event rate in CA3 and CA1. All data was normalized to pre-injury, pre-treatment levels (mean $\pm$ SEM).